Simulated effects of wet-etched induced surface roughness on IR transmission and reflection

Papatzacos, Phillip; Akram, Muhammad Nadeem; Bardalen, Eivind; Øhlckers, Per

Institute of Microsystems - University of South-Eastern Norway

Simulated effects of wet-etched induced surface roughness on IR transmission and reflection

Phillip Papatzacos
Institute of Microsystems
University of Southeastern Norway
Borre, Norway
https://orcid.org/0000-0002-2157-6282

M. Nadeem Akram
Institute of Microsystems
University of Southeastern Norway
Borre, Norway
Muhammad.N.Akram@usn.no

Eivind Bardalen
Institute of Microsystems
University of Southeastern Norway
Borre, Norway
Eivind.Bardalen@usn.no

Per Øhlckers
Institute of Microsystems
University of Southeastern Norway
Borre, Norway
Per.Ohlckers@usn.no

Abstract—**We have constructed a finite element simulation where we investigate the effects of wet-etch-induced surface roughness on transmission and reflection of infrared light in the 8-12um band. A silicon wafer was wet-etched for 2 hours in a 10% KOH solution at 80°C, scanned in an atomic force microscope, and the surface profile was recreated in COMSOL. Simulated plane waves of light and varying angles of incidence were then allowed to pass through this surface and the resulting effects on the reflection and transmission were investigated. Roughness was then amplified to investigate the effects of increased surface roughness. For the wavelengths investigated, an increase in transmission of 8% could be seen up to an RMS surface roughness of 800nm followed by a decrease, while the angles investigated showed an RMS dependent increase in transmission between 20° and 40° for RMS surface roughness' above 1000nm.**

Keywords—Wet-etching, Finite element simulation, LWIR, Silicon, Packaging, Transmission, Reflection

I. INTRODUCTION

Thermal imaging cameras have potential applications in security, manufacturing, and in the automotive industry. Price is, however, a limiting factor in most of these applications, in large part due to the sensors' packaging requirement [1, 2]. The challenge is that optical sensors are often delicate and require protection from the environment. This is even more so the case for microbolometer (MB)-based infrared (IR) sensors, which often require a high vacuum (approximately 0.1-10µbar) to operate properly [3]. One attractive way to achieve these operating conditions at large scale is to use advances in wafer-level packaging and hermetically bond a silicon-wafer with micromachined cavities to wafers with Read-Out Integrated Circuits (ROIC) and MB arrays. Using a silicon lid to enclose such a sensor is promising both due to its relatively low absorption coefficient in the Long Wave-IR (LWIR) region, its mechanical strength, and due to the fact that a wide variety of techniques has been implemented in the treatment and processing of silicon.

A commonly used technique for micromachining cavities in silicon is wet-etching in KOH. This is, however, a process that leaves some amount of roughness at the etched surfaces [4]. The effects of surface roughness on optical transmission have previously been theoretically approximated by a number of works [5, 6]. These did not, however, take into account specifics such as slope, peak sharpness, and variations in depths of valleys and heights of hills, all of which impact how much the incoming light is scattered, transmitted, and reflected. Increasing and modifying roughness to achieve lower reflectivity is also of great interest to the solar cell industry [7-9], but for these applications, image quality is of no importance and is therefore not necessarily related to optical sensors. Knowing exactly what type and what amount of roughness the MBA can tolerate at the surfaces of the lid, will help determine which processes are required for the camera to operate properly, and which can be avoided to save cost.

In this work, we are investigating the optical effects of a silicon surface with etch-induced roughness in the Finite Element (FEM) multiphysics simulation software, COMSOL. A silicon wafer was wet-etched for 2 hours in a 10% KOH solution at 80°C, which resulted in a depth of 175µm±3µm. An area of 10µm x 10µm of this surface was scanned using an atomic force microscope (Park Systems Co. AFM XE-200) with a resolution of 256x256 pixels. Lines of this surface was integrated with 2D simulations of light with wavelengths between 8µm and 12µm and incidence angles varying from 0° to 60°. The rough-surfaces' effect on transmission and reflection was studied.

II. SIMULATION

The data from the AFM scan described in the introduction was exported as points and 10 of the lines were randomly selected for our 2D simulation. From these points, a cubic spline interpolation was applied and a 2D representation of the surface was digitally recreated for each line (see figure 1). One of the strengths of our simulation lies in this accurate representation of the surface. Similar simulations of surface
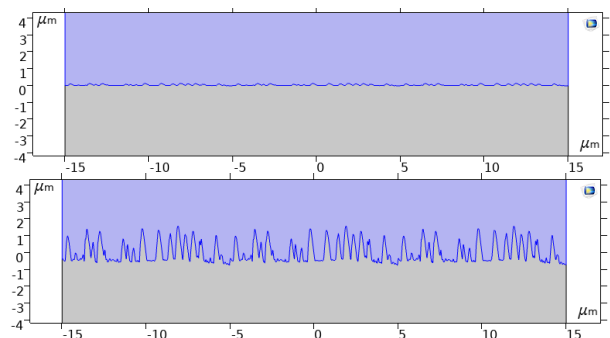

Fig. 1. Digitally recreated wet-etched silicon-air transition (top), and digitally manipulated silicon-air transition with RMS surface roughness of 580nm (bottom). Silicon in blue, vacuum in grey.

roughness and geometry on optical performance use set geometries [10] or randomly generated roughness within set parameters [11]. By copying a real-life surface, we achieve a more accurate representation of its effects. We later deviate from this real-life approximation by increasing the roughness amplitude of this surface. How this affects our simulation is commented on in the discussion section.

We have in this simulation chosen to only simulate the silicon vacuum interface (see figure 2). Un-etched polished silicon has extremely low surface roughness [4], which means the air-silicon transition is of little interest and is removed to reduce computational requirements. A 30µm wide and 90µm high rectangle is constructed with Floquet periodic conditions on both sides. Perfectly Matched Layers (PMLs) are placed on top and bottom to absorb transmitted and reflected light and thereby avoid interference. In the middle, we place a parametric surface that will define the transition from silicon to vacuum. The vacuum domain has – by definition - a refractive index of 1 while we have used [12] as a reference for the refractive index of silicon in the 8-12µm wavelength range. The features on the etched surface limited the area we could accurately measure with the AFM in a single scan to 10µm by 10µm. For the simulation to make sense, however, we need a model significantly larger than our wavelength. Therefore, to span the entire 30µm transition, the measured line is repeated thrice.
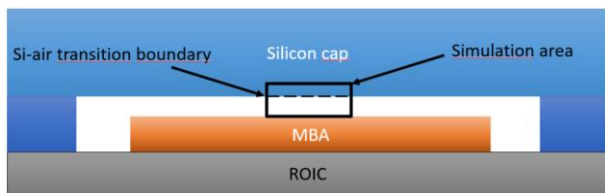

Fig. 2. Model of the entire MBA-sensor layout with simulation area highlighted

We then run 2 simulations for all 10 lines. In one simulation the angle of incidence is increased from 0°-60° in 2° increments, and in the other wavelength is increased from 8-12µm in 0.13µm increments. For every angle of incidence and wavelength, we also increase the roughness by multiplying the deviation from the zero-line – defined by our AFM scan - by an increasing integer. As a control, we run a wavelength sweep, and an angle of incidence sweep with the Si-vacuum transition perfectly flat. The results are then averaged across the 10 lines and plotted in a 3D surface diagram which is shown in the results section. The average amount of mesh elements was approximately 45 000 and the average run-time was approximately 5 hours and 15 minutes.

III. RESULTS

A. Wavelength sweep

In figure 3 we can see that the results from the wavelength sweep with increasing roughness are fairly stable, with transmission coefficient ranging from 0.66-0.8. A clear trend we can observe, however, is that there is a clear increase from 0.7 to 0.78±0.02 at RMS surface roughness of approximately 500nm. This is interesting because it is still less than $1/10^{th}$ of the minimum wavelength, which means it is unlikely to distort the image. The same peak can also be observed in the angle of incidence sweep below at 500nm at 0°.

B. Angle of incidence sweep

In figure 4 we see that as the angle of incidence increases, the transmission coefficient drops to zero at approximately 20° which corresponds to total internal reflection. An interesting observation we can make is that between 20° and beyond, an increase in RMS surface roughness actually increases our transmission coefficient. This makes intuitive
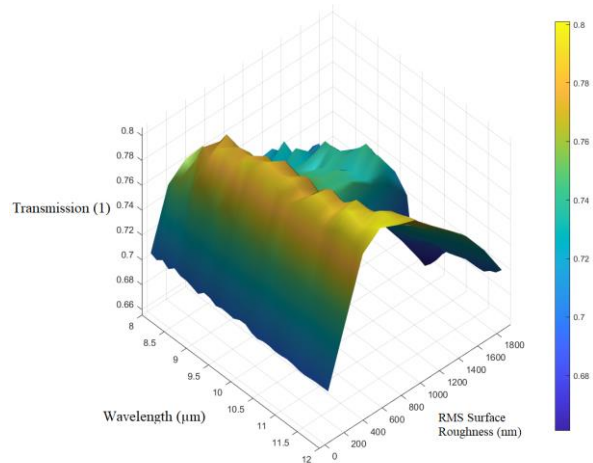

Fig. 3. Transmission coefficient as a result of increasing surface roughness and wavelength.
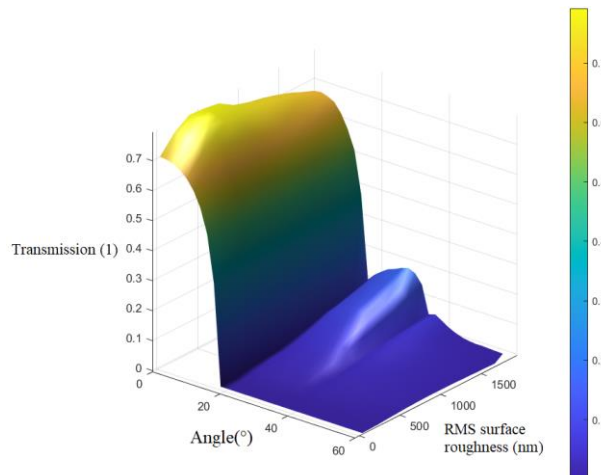

Fig. 4. Transmission coefficient as a result of increasing surface roughness and angle of incidence.

sense, considering that the increasingly sharp peaks will be more normal to light at increasing incidence angles, which aids transmission. It is worth mentioning, however, that the higher the surface roughness in this simulation, the less similar our transition is to the originally measured surface. This makes the simulated results more and more difficult to achieve in real-life.

IV. DISCUSSION

A. Surface validity

When the etched sample is studied under the microscope, some specks could be observed, which is likely reaction products deposited on the surface after etching. To mitigate this, the surface was placed, with the etched face down, in an ultrasound bath with acetone for 30 minutes. This resulted in a surface of sufficiently smooth quality.

The RMS surface roughness of our sample is calculated to be just under 38 nanometers which is an order of magnitude larger than the results achieved in [4]. This could be explained by the fact that our measured sample was etched to a depth of 175µm and theirs only to 10µm, as well as the application of a more thorough cleaning step in [4].

It is also worth noting that our digitally reconstructed 30µm surface transition is in reality a 10µm scan repeated 3 times, which could potentially lead to inaccuracies in surface representation, especially at the transition between each repetition. To investigate this, we calculate the RMS surface roughness values for the 10µm line and compare it to the 30µm line and find a decrease of $9*10^{-13}$nm in the 30µm line, which we consider negligible.

In our simulation, we also increase the roughness, simply by multiplying the z-values in our measurements. While this proportionately increases peaks and valleys, it is unclear whether this relates to real-life cases of wet-etched silicon surfaces. Considering the shape remains intact, it is, however, not unlikely, at least up to a point. The simulation will regardless shed light on the impact of roughness for transmission and reflection for varying angles of incidence and wavelengths in the LWIR region.

B. Simulation validity

While simulation is never a substitute for the real thing, it can demonstrate or highlight problems in a manufacturing process early and cost-effectively, provided the simulation accurately reflects real life. One very important consideration that may affect this validity in FEM simulations like this one is mesh-element size. A general rule of thumb is to have mesh elements no bigger than a fifth of the wavelength. To air on the side of caution, we have chosen a maximum mesh size of 0.8µm which is a tenth of our minimum wavelength. We have also specified a small region surrounding our transition where the mesh size is defined to be a minimum 1.5pm, which is a third of the minimum measured deviation, and maximum 188nm, which is the maximum measured deviation. This is done to ensure that the transition is properly rendered.

Another step taken as a measure of validity is to add up the total of the simulated reflection, transmission, and absorption. In a valid simulation, these fractions should theoretically add up to unity. The plots are shown in figures 5 and 6 and we see that the simulation does this, especially at lower roughness' and angles.

A final step taken to validate our simulation is to compare our simulation of a smooth transition to an analytic estimation. For perfectly smooth surfaces the theoretical reflectance of the surface given by Fresnel's equation:

$$R_{analytic} = \left(\frac{n_1 Cos(\theta_i) - n_2 Cos(\theta_t)}{n_1 Cos(\theta_i) + n_2 Cos(\theta_t)}\right)^2 \qquad (1)$$
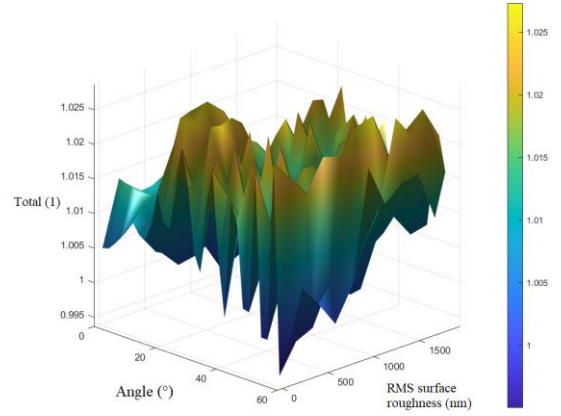

Fig. 5. Control showing the sum of transmission, reflection and absorption for roughness angle sweep
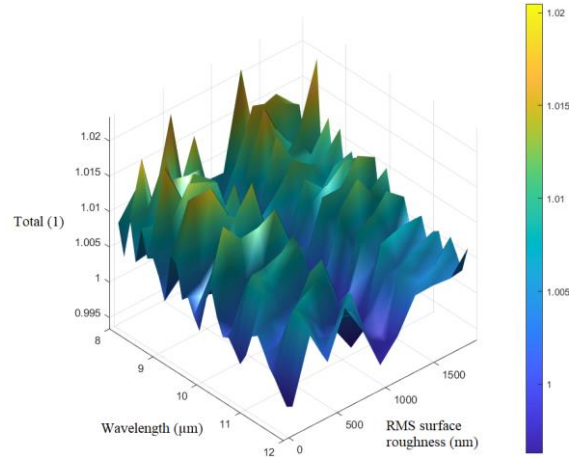

Fig. 6. Control plot showing the sum of transmission, reflection and absorption for roughness and wavelength sweep

Equation (1) may be rewritten as:

$$R_{analytic} = \left(\frac{n_1 Cos(\theta_i) - n_2 \sqrt{1 - \left(\frac{n_1}{n_2}\sin(\theta_i)\right)^2}}{n_1 Cos(\theta_i) + n_2 \sqrt{1 - \left(\frac{n_1}{n_2}\sin(\theta_i)\right)^2}}\right)^2 \qquad (2)$$

Where n_1 and n_2 are the refractive indices of the two materials in the transition, and θ_i and θ_t is the angle of incidence and transmittance respectively. The analytic results from equation (2) are plotted with the simulated results in figure 7 and we see near-perfect overlap between the plots.

V. CONCLUSION AND OUTLOOK

We have constructed a simulation of LWIR light hitting a wet-etched silicon surface with more accuracy than previous works. We have also investigated how increasing RMS surface roughness affects a surface with this topography with regards to transmission and reflection. We can with confidence say that for LWIR light with wavelength 8-12µm, wet-etch induced roughness is not a concern when it comes to
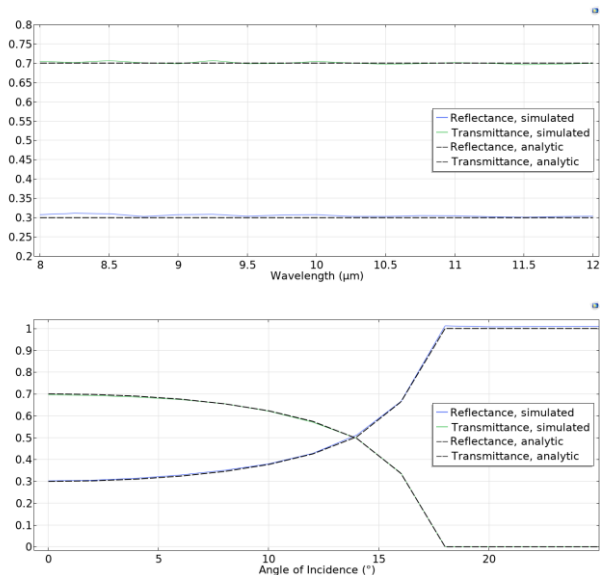
Fig. 7. Comparison of analytic and simulated results for reflectance and transmittance of a flat surface silicon-air transition. Data beyond 25° has been remover as the results are the same from 20° upwards

reflection and transmission, especially considering our high RMS values compared to other wet-etch analyses.

We have also reported that for angles between 20° and 40°, higher surface roughness may actually lead to lower reflection and higher transmission than a smoother surface. For wavelengths between 8μm and 12μm, we saw a peak in transmission at approximately 500nm surface roughness. This will be experimentally verified in further work and could lead to possible implementations as anti-reflective topographies in optical systems e.g. solar cells and thermal cameras.

Most importantly, however, we have constructed and demonstrated a simulation framework that may be used for a multitude of surfaces, wavelengths, incidence angles, and materials, with more accuracy than previous simulation work and with less physical requirements than experimentation. This simulation will also be expanded to make estimations with simple anti-reflective coatings, and the effect of surface roughness on converging light beams, to give insight into the roughness' effect on image quality.

[1] H. Liu, G. Salomonsen, K. Wang, K. E. Aasmundtveit, and N. Hoivik, "Wafer-level Cu/Sn to Cu/Sn SLID-bonded interconnects with increased strength," (in English), *IEEE Trans. Compon. Packag. Manufact. Tech.,* Article vol. 1, no. 9, pp. 1350-1358, 2011, Art no. 5967893, doi: 10.1109/TCPMT.2011.2156793.

[2] A. Decharat, "Integration and Packaging Concepts for Infrared Bolometer Arrays," KTH, 2009.

[3] A. Hilton *et al.*, "Wafer-level vacuum packaging of microbolometer-based infrared imagers," in *Proceedings of the International Wafer-Level Packaging Conference, San Jose, CA, USA*, 2016, pp. 19-20.

[4] S. Chandrasekaran and S. Sundararajan, "Effect of microfabrication processes on surface roughness parameters of silicon surfaces," *Surf. Coat. Technol.,* vol. 188, pp. 581-587, 2004.

[5] R. Swanepoel, "Determination of surface roughness and optical constants of inhomogeneous amorphous silicon films," *Journal of Physics E: Scientific Instruments,* vol. 17, no. 10, p. 896, 1984.

[6] P. Bussemer, K. Hehl, and S. Kassam, "Theory of light scattering from rough surfaces and interfaces and from volume inhomogeneities in an optical layer stack," *Waves in random media,* vol. 1, no. 4, pp. 207-221, 1991.

[7] N. Zin *et al.*, "Polyimide for silicon solar cells with double-sided textured pyramids," *Solar Energy Materials and Solar Cells,* Article vol. 183, pp. 200-204, 2018, doi: 10.1016/j.solmat.2018.03.015.

[8] M. K. Basher, M. K. Hossain, M. J. Uddin, M. A. R. Akand, and K. M. Shorowordi, "Effect of pyramidal texturization on the optical surface reflectance of monocrystalline photovoltaic silicon wafers," *Optik,* Article vol. 172, pp. 801-811, 2018, doi: 10.1016/j.ijleo.2018.07.116.

[9] M. K. Basher, M. K. Hossain, and M. A. R. Akand, "Effect of surface texturization on minority carrier lifetime and photovoltaic performance of monocrystalline silicon solar cell," *Optik,* Article vol. 176, pp. 93-101, 2019, doi: 10.1016/j.ijleo.2018.09.042.

[10] Y. F. Makableh, M. Al-Fandi, M. Khasawneh, and C. J. Tavares, "Comprehensive design analysis of ZnO anti-reflection nanostructures for Si solar cells," *Superlattices and Microstructures,* vol. 124, pp. 1-9, 2018.

[11] J. Borneman, A. Kildishev, K.-P. Chen, and V. Drachev, "FE modeling of surfaces with realistic 3D roughness: Roughness effects in optics of plasmonic nanoantennas," in *Proceedings of the COMSOL conference 2009 Boston*, 2009.

[12] D. Chandler-Horowitz and P. M. Amirtharaj, "High-accuracy, midinfrared (450 cm−1⩽ ω⩽ 4000 cm−1) refractive index values of silicon," *Journal of Applied physics,* vol. 97, no. 12, p. 123526, 2005.